FRA-73-12

REPORT NO. FRA-ORD&D-74-24

INPUT POWER CHARACTERISTICS OF THE THYRISTOR VARIABLE VOLTAGE POWER CONDITIONER

John J. Stickler
George P. Ploetz
Frank L. Raposa

NOVEMBER 1973

FINAL REPORT

Prepared for:
DEPARTMENT OF TRANSPORTATION
URBAN MASS TRANSPORTATION ADMINISTRATION
Office of the Administrator
Washington D C 20590

Technical Report Documentation Page

1. Report No.	2. Government Accession No.	3. Recipient's Catalog No.
FRA-ORD&D-74-24		

4. Title and Subtitle	5. Report Date
INPUT POWER CHARACTERISTICS OF THE THYRISTOR VARIABLE VOLTAGE POWER CONDITIONER	November 1973
	6. Performing Organization Code
7. Author(s) John J. Stickler, George P. Ploetz and Frank L. Raposa	8. Performing Organization Report No. DOT-TSC-FRA-73-12
9. Performing Organization Name and Address Department of Transportation Transportation Systems Center Kendall Square Cambridge MA 02142	10. Work Unit No. (TRAIS) UM401/R4701
	11. Contract or Grant No.
12. Sponsoring Agency Name and Address Department of Transportation Urban Mass Transportation Administration Office of the Administrator Washington DC 20590	13. Type of Report and Period Covered Final Report Oct. 1972 - June 1973
	14. Sponsoring Agency Code

15. Supplementary Notes

16. Abstract

A laboratory study was made of transformer and thyristor voltage control for speed control of a rotary induction motor. The test program consisted of two parts; the first dealing with measurements of the induction motor characteristics and the second with the distribution of complex electric power in the system with both types of voltage-control. The current harmonics which are generated by thyristor control are shown to give rise to additional motor losses and reduction in motor efficiency. The non-sinusoidal currents present with thyristor control produce reactive distortion power. Suggestions are made regarding the suitable instrumentation to use in measuring the distortion power as well as the other components of complex power in the system

17. Key Words	18. Distribution Statement
· Thyristor Control · Variable Voltage Power Conditioner · Linear Induction Motors	DOCUMENT IS AVAILABLE TO THE PUBLIC THROUGH THE NATIONAL TECHNICAL INFORMATION SERVICE, SPRINGFIELD, VIRGINIA 22151.

19. Security Classif. (of this report)	20. Security Classif. (of this page)	21. No. of Pages	22. Price
Unclassified	Unclassified	50	

Form DOT F 1700.7 (8-72) Reproduction of completed page authorized

PREFACE

The laboratory study described in this report was performed in the Power and Propulsion Branch of the Transportation Systems Center (TSC) for the Urban Mass Transportation Administration (UMTA) as part of the Urban Tracked Air Cushion Vehicle (UTACV) Programs. The objective of this work was to determine the input power characteristics of thyristor controlled induction motors.

TABLE OF CONTENTS

LIST OF ILLUSTRATIONS

LIST OF TABLES

LIST OF SYMBOLS

I_1'	- RMS line current
$I_1'(n)$	- RMS line current harmonic of order n
i_1	- instantaneous line current
n	- order of harmonic
P_r	- active power, watts
P_m	- mechanical power, watts
P_n	- mechanical power harmonic of order n
Q_p	- reactive displacement power, voltamperes
Q_d	- reactive distortion power, voltamperes
Q_t	- total reactive power, voltamperes
S	- apparent power, voltamperes
s	- motor slip
T	- motor torque
V_1'	- RMS input line voltage
V' (n)	- RMS voltage harmonic of order n
V_2'	- RMS load voltage
v_2	- instantaneous voltage
W_1, W_2	- wattmeter readings
α	- thyristor (firing) delay angle, radians
ϕ	- fundamental power factor angle, radians
ϕ_n	- harmonic power factor angle, radians
θ	- system power factor angle
η	- motor efficiency

1. INTRODUCTION

Thyristors are being increasingly utilized for the control of induction machines in system applications. One example of this is the thyristor control system specified for use with the linear induction motor in the Urban Tracked Air Cushion Vehicle (UTACV).[1] The advantages of this solid state control system which make it particularly suited for speed control applications are related to ease of operation and maintenance, as well as overall reliability.

It is desirable when considering the application of a particular power conditioning system to have data relating the power conditioning process to the relative distribution of electrical power (complex) in the system. This applies especially to thyristor-control since the control process results in a different distribution of electrical power in the system than occurs for the case of transformer-control. Reactive distortion power, generated as a by-product of thyristor-control, must be accommodated in the system in addition to the real and reactive displacement powers. A study of the relations governing the balance between the different components of complex power is warranted and constitutes a further objective of this report.

Closely related to the matter of the complex power in the electrical system is the question of the most suitable electrical instrumentation to use in monitoring the system power characteristics. The presence of higher harmonics with thyristor control affects the choice of electrical instrumentation. The accuracy of the power measurements conducted when both current and voltage higher harmonics are present in the system is discussed later in the report.

A survey of the literature reveals numerous papers dealing with various aspects of thyristor-control including its application to speed-control of rotary induction motors. Paice[2] examined the characteristics of various types of thyristor control circuits in an attempt to determine the best control circuit for three-phase motors. Shepard and Stanway[3] study the torque-speed

characteristics of delta and wye connected induction motors controlled by series thyristor switches and presented measured results of the motor performance versus relative harmonic content. The effect of nonsinusoidal voltage and current wave forms on induction motor characteristics was examined in more detail by Chalmer[4] et. al, Klingshirm and Jordan,[5] and Jain.[6] Lipo[7] presented a theoretical analysis of an induction motor controlled by symmetrically triggered thyristors and obtained computed solutions for the phase current waveforms and motor torque which agreed very closely with experiment. Based on the above analysis, Stickler[8] developed a computer program which evaluated exact mathematical expressions for the induction motor currents with thyristor control. Other papers dealing with theoretical analyses of thyristor-controlled induction motors include those by Bedford and Nene,[9] Novotny and Fath,[10] and Shepherd.[11]

The problem of power factor measurements has been discussed by Schmidt.[12] Erlicki[13] et. al. examined the errors which result in power measurements when the line currents are discontinuous. A more general treatment of instrumentation in the presence of nonsinusoidal currents has been given by Stanton.[14]

The general subject of complex power in terms of real, displacement, and distortion powers is treated in the text by Schaeffer.[15] A more detailed analysis of the reactive power in the presence of nonsinusoidal currents and voltages has been presented by Shepherd.[16] The latter paper points out the fallacy of the expression normally used to describe reactive displacement power and gives new expressions for the power components which lead to a consistent interpretation of complex power.

Survey papers dealing with power conditioning for high speed ground transportation vehicles have been published by Raposa[17] and Cacossa.[18]

The subject matter in the report is divided into two parts. The first part deals with a laboratory study of the output characteristics of a rotary induction motor using transformer and thyristor-voltage-control. The motor efficiencies with both types of

voltage control are examined from zero to rated motor speed. The second part addresses the subject of complex power in the electrical system and the proper instrumentation to use in measuring power in transformer and thyristor-voltage-control systems. The conclusions in the final section summarize the results of the comparative study of thyristor and transformer-voltage-control systems and gives recommendations on the most suitable type of instrumentation to be used in measuring the system power characteristics of voltage-controlled induction motors.

2. TECHNICAL DISCUSSION

2.1 REVIEW OF TRANSFORMER-AND THYRISTOR-VOLTAGE CONTROL SYSTEMS

2.1.1 Transformer-Voltage-Control

A method of transformer-voltage-control for regulating the electrical power fed to a load utilizes a ganged-three-phase variable voltage auto transformer for controlling the output voltage. In contrast to the method of thyristor-control, no intermediary power conditioning unit is required between the power source and load. Since there is no distortion of the input power associated with the voltage control, the apparent power, S, given by the sum of the product of RMS phase voltage and line current is simply,

$$S^2 = (Q_p^2 + P_r^2) \qquad (1)$$

where Q_p is the displacement power and P_r is the active input power to the load. The absence of higher frequency harmonics accompanying the power conditioning process simplifies the task of measuring the electrical system parameters. The electrical instruments required to measure the current, voltage, and input power quantities need not be wide-band but must only respond accurately at the fundamental frequency of the power source.

The electrical quantities which are measured in the laboratory investigation of transformer voltage control are listed below.

TABLE 1 EMPIRICAL PARAMETERS MEASURED WITH TRANSFORMER-CONTROL

V_1' - input supply voltage (line-to-line)

I_1' - line current

V_2' - load voltage (line-to-line)

W_1 - input power

W_2 - input power

The related electrical quantities which are derived from data taken on the above parameters are given below.

P_r - (real) active power

Q_p - (reactive) displacement power

S - apparent power

$\cos\theta$ - system power factor

The real and displacement powers are evaluated by the standard two-wattmeter method using the wattmeter data W_1, W_2.

2.1.2 Thyristor-Voltage-Control

The power conditioning unit with thyristor-control is illustrated in the sketch shown in Figure 1. The basic control unit consists of 3 pairs of back-to-back thyristors which are symmetrically triggered by an auxilliary triggering unit. Each thyristor turns on when both a forward voltage and a triggering signal are applied, and turns off when the load current decreases to zero. Control of the power fed to the load is accomplished by varying the delay angle of the trigger signal relative to the input driving voltage.

The independent electrical parameters describing the operating state of the thyristor control system are as follows:

I_1' = phase current (RMS)

V_1' = input line-to-line voltage (RMS)

V_2' = output line-to-line voltage (RMS)

α = (thyristor firing) delay angle

The primed current and voltage quantities are RMS and include the fundamental plus higher frequency harmonic components. The delay angle, α, is illustrated in Figure 2 for a typical example of instantaneous voltage and current waveforms. α is defined[19] as the interval in electrical degrees by which the firing pulse is delayed by phase control in relation to natural operation that would occur with no controller circuit elements in the circuit and a purely resistive load.

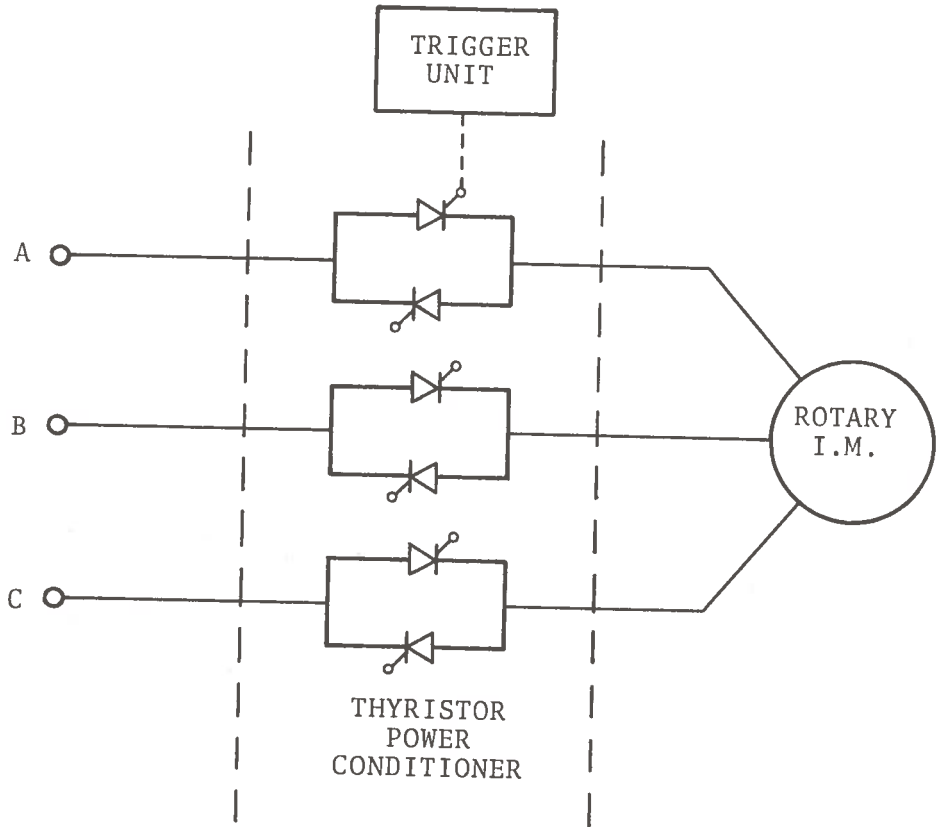

Figure 1 Schematic of Thyristor Power Conditioner

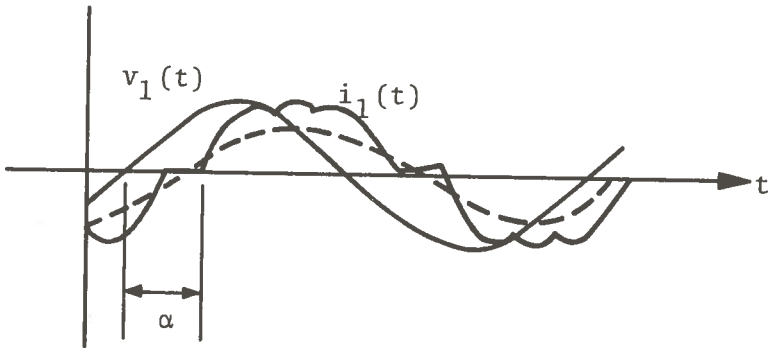

Figure 2 Current-Voltage Waveforms with Thyristor-Control

If the instant of zero input phase voltage is taken as a reference, the instantaneous input (line-to-line) voltage can be written as

$$v_1(t) = \sqrt{2}\, V_1' \sin(\omega t) \tag{2}$$

For the conditions applicable to thyristor-control[1] it has been shown that the instantaneous phase current and output phase voltage can be expressed by the sum of three time-dependent terms, consisting of one sinusoid plus two damped-sinusoids. It is customary, however, to write the instantaneous current and voltage as a Fourier series of harmonic terms of order n.

$$i_1(t) = \sum_n \sqrt{2}\, I'(n) \sin(n\omega t - \phi_n) \tag{3}$$

$$v_2(t) = \sum \sqrt{2}\, V'(n) \sin(n\omega t - \beta_n) \tag{4}$$

where $I'(n)$, $V'(n)$ are the current and voltage harmonic amplitudes (RMS) and ϕ_n and β_n are the corresponding phase angles, referenced to the position of zero input voltage crossing, associated with the harmonic components. Expressed in terms of the harmonic amplitudes, the root-mean-squared current and voltage are given by,

$$I_1' = \sqrt{\sum_n I'^2(n)} \tag{5}$$

$$V_2' = \sqrt{\sum V'^2(n)} \tag{6}$$

The apparent power, S, is equal to the product of the RMS input voltage, V_1, and line current, I_1.

$$S = V_1' \cdot I_1'$$

$$= \sqrt{V_1'^2 \sum_n I'^2(n)} \tag{7}$$

Expanding the series under the radical sign yields,

$$S = \sqrt{V^2\left[I'^2(1)\cos^2\phi, + I_1'^2(1)\sin^2\phi, + I'^2(3) + I'^2(5) + I'^2(7)+\ldots\right]}$$

$$= \sqrt{P_r^2 + Q_p^2 + Q_d^2} \qquad (8)$$

where

$$P_r = V_1' \; I'(1) \cos(\phi) \text{ Effective Power} \qquad (9)$$

$$Q_p = V_1' \; I'(1) \sin(\phi_1) \text{ (Displacement Power)} \qquad (10)$$

$$Q_d = V_1' \sqrt{I'^2(3) + I'^2(5) + I'^2(7) + I'^2(9) + \ldots}$$

(Distortion Power) (11)

The above three equations express the active power P_r, displacement power, Q_p, and distortion power, Q_D, in terms of the amplitude (RMS) of the Fourier harmonic components of current and voltage. In a 3-dimensional representation in which P_r, Q_p, Q_D are the power components along the three orthoginal axes, S is given by the vector sum of the orthoginal components.

The average power input to the system is also equal to the effective power, P_r. Thus

$$P_r = \frac{1}{2\pi}\int_0^{2\pi} v_1(t) \cdot i_1(t) \, d\omega t \qquad (12)$$

$$= \frac{1}{\pi}\int_0^{2\pi} V_1' \sin \omega t \cdot \sum_n I'(n) \sin(n\omega t - \phi_n) d\omega t$$

$$= V_1' \; I'(1)\cos\phi_1$$

The displacement power represents the reactive power associated with the fundamental current component in quadrature with the applied input voltage. The distortion power as given by Equation (14) illustrates the dependence of this form of reactive power on the higher

Fourier harmonics generated in the thyristor-voltage-control process. An alternate expression for distortion power in terms of true RMS current, I_1' and fundamental current harmonic, I'(1), is

$$Q_d = V_1' \cdot \sqrt{I_1'^2 - I'(1)^2} \qquad (13)$$

The distortion power represent the price which must be paid in terms of additional stored electrical energy for the use of thyristor-control.

The total input reactive power, Q_T, is defined[15] as the vector sum of the reactive displacement power and distortion power. It is given by the relation

$$Q_t = \sqrt{Q_p^2 + Q_d^2} \qquad (14)$$

The power components discussed above and described by Equations (9), (10), and (11) refer to power quantities at the input to the power conditioning unit. The real power measured at the input terminals of the load will be equal to the real component of input system power, given by Equation (12), minus the real power absorbed in the power conditioning unit. The displacement and distortion powers at the input to the load are not described by equations of the form of Equations (13) and (14). For further details regarding the definition of reactive powers when both current and voltage harmonics are present, the reader is referred to Reference 16.

2.2 INDUCTION MOTOR OUTPUT PARAMETERS

2.2.1 Induction Motor Efficiency Using Transformer-Control

A brief summary of the output parameters characterizing a rotary induction motor will now be presented. These parameters include the mechanical power developed by the motor, P_m, the real power consumed by the motor, P, and the motor efficiency, η.

The mechanical power developed by a three-phase induction motor is equal to the power dissipated in an effective rotor resistance $R_2(1-s)/s$ or

$$P_m = 3\, I_2'^2 R_2 (1-s)/s \qquad (15)$$

where I_2' is the current in the secondary (rotor) circuit and s is the motor slip.

The total real power input to the induction motor load is the sum of the heating I^2R losses in primary (stator) and secondary circuits, the mechanical output power, and the additional power losses due to friction and windage.

$$P_r = I_1'^2 R + I_2'^2 R_2 + P_m + P_{friction} + P_{windage} \qquad (16)$$

The motor efficiency, by definition, is given by the ratio of useful output power to total real (effective) power input or,

$$\eta = P_m/P_r \qquad (17)$$

2.2.2 Induction Motor Efficiency Using Thyristor-Control

The output parameters for the case of thyristor-voltage control take a somewhat different form than for the case of transformer-voltage-control due to the presence of additional higher harmonic components in the current waveform. The mechanical power developed by the three-phase induction motor equals the sum of the individual mechanical harmonic powers, if account is taken of the negative torques associated with the 3n-1 th harmonics.

$$P_m = P_m(1) - P_m(5) + P_m(7) - P_m(11) + \ldots \qquad (18)$$

Each harmonic amplitude of mechanical power, $P_m(n)$, has the form of Equation (2) with I_2 now replaced by the secondary harmonic current amplitude (RMS), $I_2'(n)$, and the slip, s, replaced by the effective slip, s*, given by

$$S^* = \frac{n-1+s}{n} \qquad n = 1, 7, 13, 19, \ldots \qquad (19)$$

$$S^* = \frac{n+1-s}{n} \qquad n = 5, 11, 17, 23, \ldots$$

The torque, T, is given by

$$T = \frac{P_m}{\omega(1-s)} \qquad (20)$$

The motor efficiency, η, is equal to the ratio of output mechanical power to the real power input, P_r, according to Equation 17. When expressed in terms of the Fourier harmonic components it takes the form,

$$\eta = \frac{P_m(1)-P_m(5)+P_m(7)-\ldots}{\sum I_1'^2(n)R_1+\sum I_2'^2(n)R_2+P_{friction}+P_{windage}+P(1)-P(5)+P(7)-\ldots} \quad (21)$$

The motor efficiency with thyristor-voltage-control will be less than with transformer-voltage-control since the mechanical power harmonics alternate in sign while the heating loss terms in the denominator remain positive. Further, the mechanical power harmonics tend to approach zero at higher harmonic orders since the effective slips given by Equation (19) approaches unity for large n. The effect of the harmonic power losses is generally not serious enough to impair the use of thyristor-control in most practical applications however, it is a factor which should be taken into consideration when designing a power control system for efficient power utilization.

The power factor angles relating the components of complex input power to the system are illustrated in the vector diagram given in Figure 3. The fundamental active power, P_r, fundamental displacement power, Q_p, and distortion power, Q_d, are indicated by vectors drawn along a set of three orthoginal axes. The input displacement power factor angle, ϕ, is the angle between the fundamental active power and the apparent power of the fundamental. The input displacement power factor, cos ϕ, is evaluated from the two-wattmeter measurements of effective and displacement powers according to the relation,

$$\cos \phi = P_r/(P_r^2 + Q_p^2)^{\frac{1}{2}} \quad (22)$$

or alternately it can be found by direct measurement of the phase angle displacement between the fundamental voltage and current waveforms using a tuned phase sensitive detector. With the application of thyristor-control and the generation of distortion power, it is convenient to define a system power factor angle, θ, representing the angle between the fundamental active power, P_r, and the total apparent power (voltampere input) to the system, S. The system power factor, cos θ, is then given by,

$$\cos \Theta = P_r/S \qquad (23)$$

It is determined from measurements of the effective power by the standard two-wattmeter method plus RMS measurements of input voltage and line current.

A summary of the electrical quantities which are measured in the laboratory study of thyristor-control is listed below. In addition to the parameters given in Table 1. the list includes the power measured both at the input to the thyristor-control unit and at the load, as well as the amplitudes of the first 6 current, and voltage harmonics.

TABLE 2 EMPIRICAL PARAMETERS MEASURED WITH THYRISTOR-CONTROL

V_1 - supply voltage (line-to-line)

I_1 - line current

V_2 - load voltage (line-to-line)

W_1 - input output power

W_2 - input output power

I(1), I(5), I(7), I(11), I(13), I(17)

V(1), V(5), V(7), V(11), V(13), V(17)

α - (thyristor firing) delay angle

A list of quantities computed from data taken on the above parameters is summarized below.

P_r - active (real) power

Q_p - displacement power (reactive)

Q_d - distortion (reactive) power

S - apparent power

cosΘ - system power factor (includes effect of distortion power)

cosϕ - displacement power factor

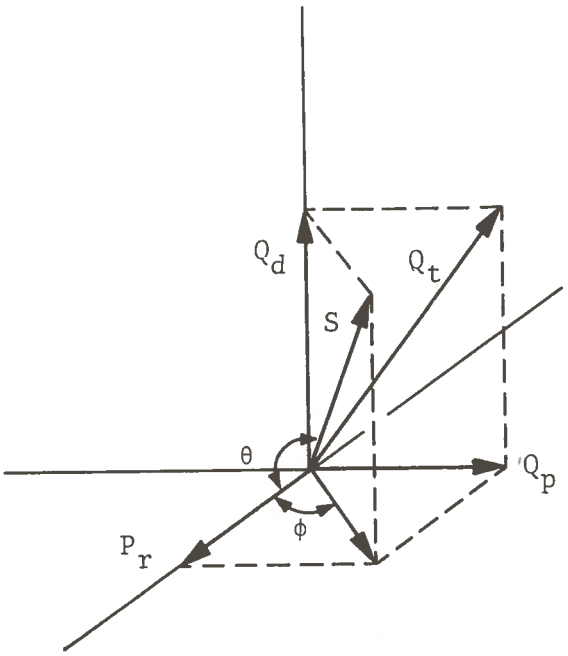

Figure 3 Vector Representation of Complex System Power

2.3 LABORATORY STUDY OF TRANSFORMER-CONTROLLED-SYSTEMS

The laboratory test setup used to compare the system characteristics of a transformer-voltage-controlled induction motor with that of a thyristor-voltage-controlled induction motor is illustrated by the block diagram given in Figure 4. AC power from a 220 volt, three-phase line source is fed to the power conditioning unit. The controlled output voltage from the conditioner drives a 3-phase rotary induction motor serving as the output load. The mechanical power developed by the load is regulated by controlling the motor torque using a water brake dynanometer.

The rotary induction motor used in the laboratory investigation was a Class D Howell Electric motor, Type FZ, having a rated output of 15 hp at 1550 rpm. The windings are 3-phase Wye connected. At rated load, the motor slip is 0.14 and line current is 44 amperes. The stator winding was modified to provide external access to the neutral Wye junction.

The water-brake dynanometer was the 90 hp Stuska Model 90413. The braking torque developed by the dynanometer is adjustable by controlling the rate of water flow through the absorption brake. The accuracy of the dynanometer output instrumentation was estimated to be 4 percent in the higher speed range. Output meter fluctuation in the lower speed range reduced somewhat the resolution of the output readings at low speeds.

The laboratory investigation of transformer-voltage-control as applied to an induction motor load was divided into two parts. The first part deals with measurements of the output characteristics of the induction motor at constant current over the operating speed range of the motor. Such measurements are required to evaluate the power characteristics of the induction motor load. The second part is devoted to a analysis of transformer voltage-control and treats the various real and reactive powers in the control system. This latter part lays the foundation for a subsequent comparative study of the transformer-versus-thyristor voltage control methods.

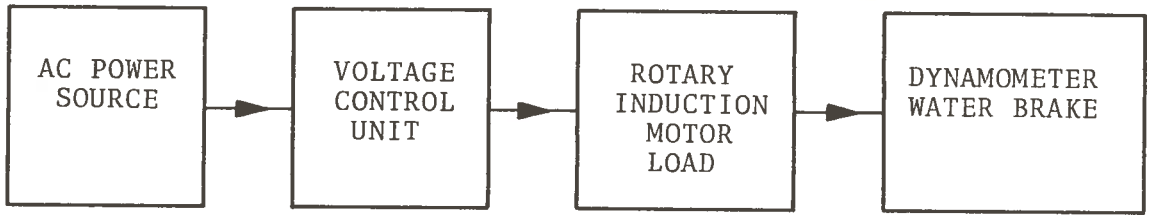

Figure 4 Block Diagram of Laboratory Test Setup

2.3.1 Output Power Characteristics

The investigation of transformer-voltage-control as applied to an induction motor load begins with a brief laboratory study of the output characteristics of the Howell induction motor when operated with constant stator current excitation. This study has two purposes, first, it provides data which can be used as a basis for deriving the equivalent circuit of the induction motor load. Second, it furnishes information which can be used to compare the output power characteristics of the induction motor using transformer-voltage-control with similar characteristics obtained using thyristor-voltage-control.

Test data was taken on active input power, P_r, mechanical output power, P_m, and apparent power, S, as a function of motor speed for the fixed rated motor current of 44 amperes. The input voltage V_2, and dynanometer load were adjusted coincidentally to maintain the stator current constant during the course of the tests. The data was taken in speed increments of 125 rpm over the range of rotor speed from 0 to 1550 rpm. The real power input was measured by the standard two-wattmeter method and the mechanical power was measured directly by calibrated instruments incorporated as an integral part of the Stuska dynanometer.

Figure 5 presents the output characteristics of the Howell induction motor as a function of rotor speed for rated current of 44 amperes. The displacement power factor and motor efficiency computed using Equations (22) and (17) respectively are also presented for completeness. The effective power and mechanical power increase with motor speed. Since the effective power and mechanical power must ultimately decrease as motor speed approaches zero slip, a maximum in the effective and mechanical powers should occur at speeds higher than those measured.

The equivalent impedance parameters were previously[8] determined from blocked-rotor and no-load tests plus static measurements of the DC input resistance. Based on these parameters, the I^2R losses in the stator and rotor circuits were computed. The dashed curve gives the sum of these I^2R losses and the mechanical output

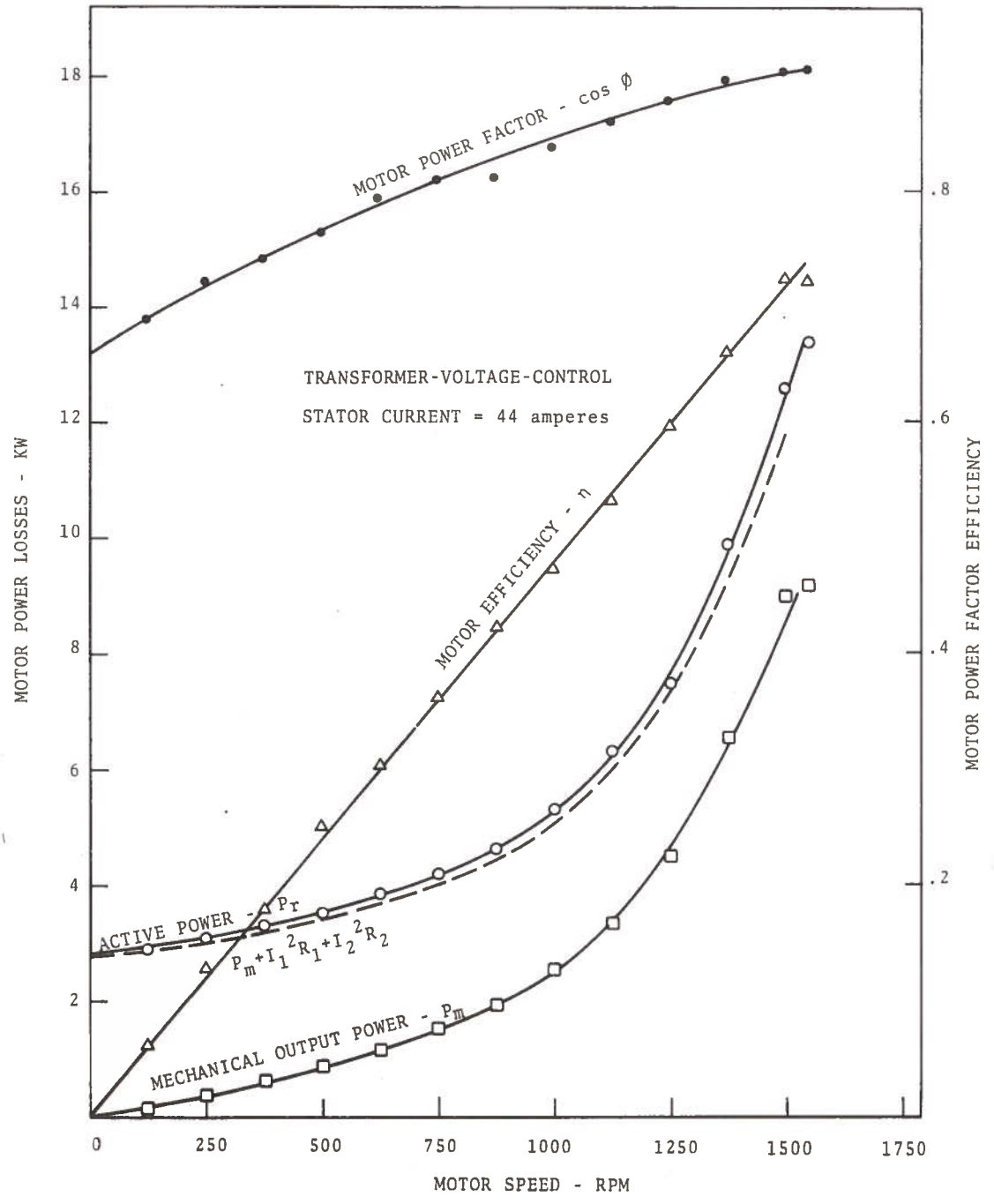

Figure 5 Induction Motor Characteristics with Transformer-Voltage-Control

power. The difference between the dashed curve and the curve of effective power represents the power consumed in overcoming frictional and windage losses.

The motor efficiency increases approximately linearly with speed and at 1550 rpm reaches a peak efficiency of 72.8 percent. Since motor efficiency is zero at synchronous speed (slip = 0), a peak in motor efficiency must likewise occur in the speed range lying between the upper speed limit and synchronous speed. The power factor varies from 0.66 at standstill to 0.90 at 1550 rpm. The comparatively high power factor measured at standstill is characteristic of Class D type motors.

2.3.2 Input Power Characteristics

The components of electrical power in the transformer-voltage-control system is illustrated in Figure 6 where input apparent power, S, active power, P_r, and reactive displacement power, Q_p, are plotted against motor speed. Since distortion power is absent in transformer-control, the displacement power is equal to the total reactive power. The measurement of effective and reactive power was accomplished by the standard two-wattmeter method. All measurements were made at constant stator current of 44 amperes.

The effective power, P_d increases from a minimum value at standstill equal to 3 kw to a peak value of 13.4 kw at rated speed. The predominant factor causing the increase in effective power-versus-speed is the steady increase in mechanical power with speed. See Figure 5. Ultimately the effective power input to the load must decrease since both the mechanical output power and rotor heating I^2R losses must approach zero at synchronous speed. A maximum in the effective power absorbed by the load must take place for some speed lying between that of the highest speed measured and synchronous speed.

The reactive power, Q_p, representing the nonuseable power in time quadrature with the real power, is observed to increase from 2.9 kvar at standstill to 6.4 kvar at 1550 rpm. At unity slip or standstill, the reactive power is almost equal to the real power

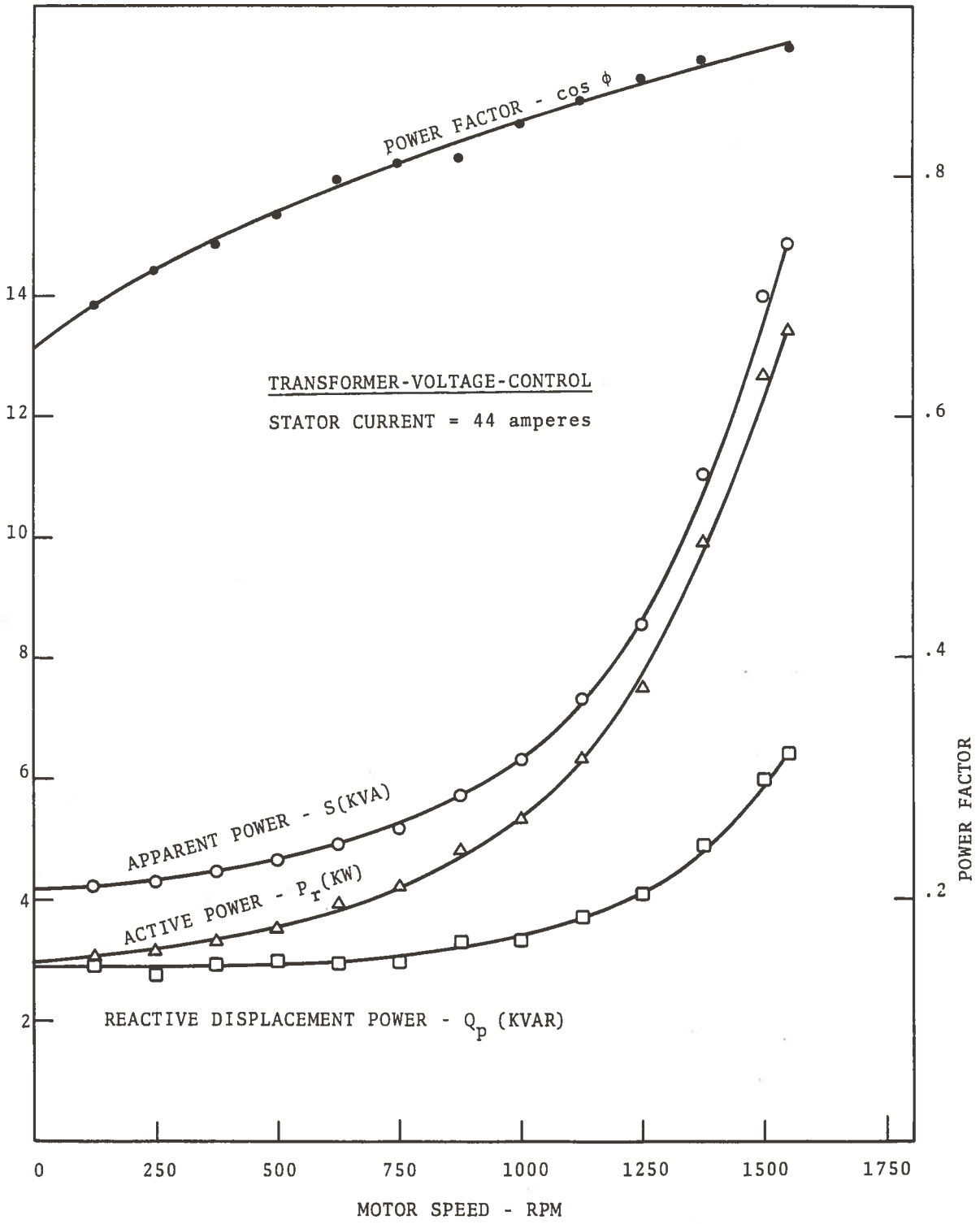

Figure 6 Power System Characteristics with Transformer-Voltage Control

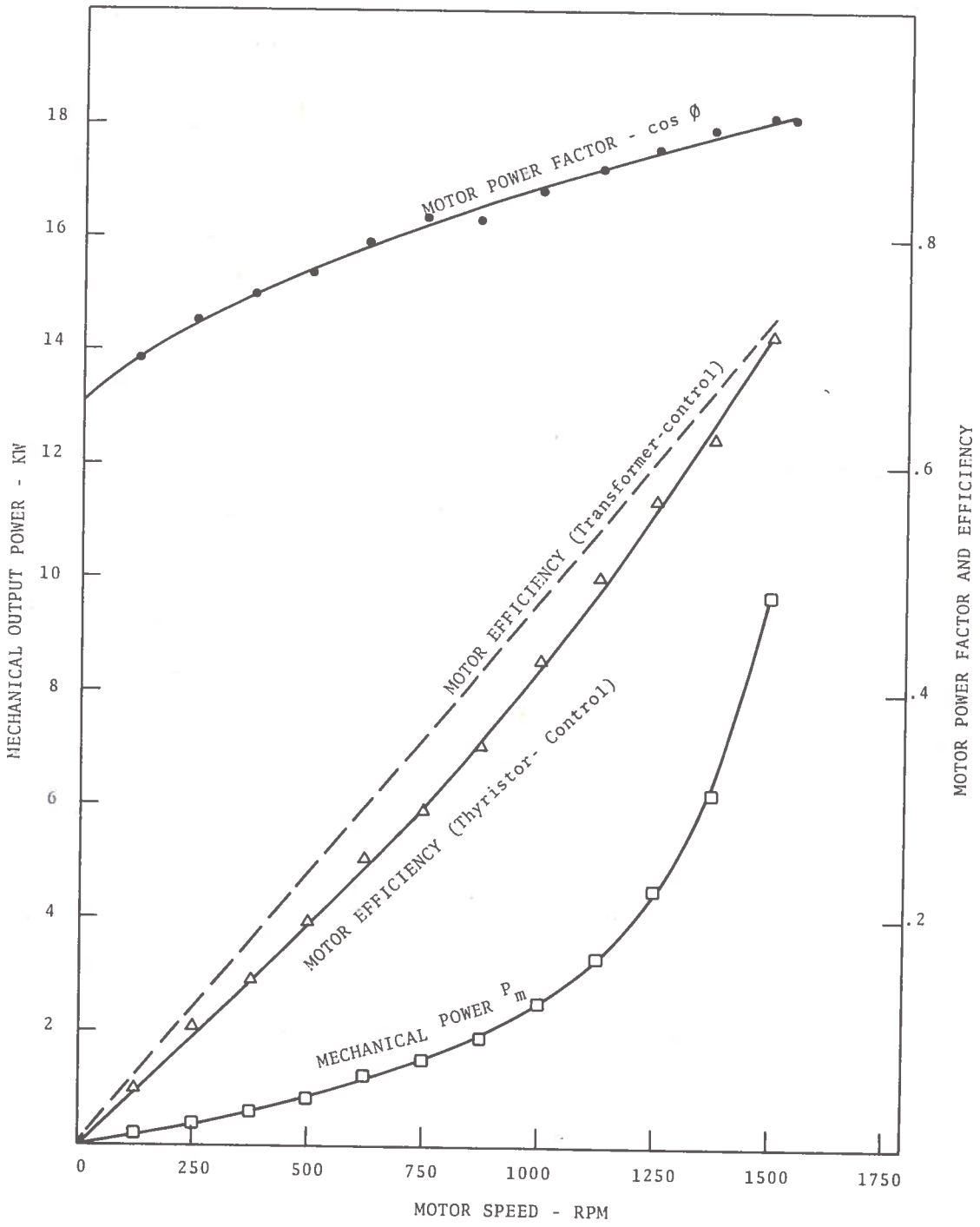

Figure 7 Induction Motor Characteristics With Thyristor-Voltage-Control

are zero at zero speed and are nearly equal at the upper speed limit of 1500 rpm. Since thyristor current blocking is effectively reduced to zero in the upper speed limit, the difference in efficiencies is due solely to the I^2R losses in the thyristor-control unit amounting to 360 watts. Additional deviation at lower speeds is the result of the reduced mechanical output power caused by the presence of higher-harmonic currents in the rotor circuit. At the speed of 750 rpm, the motor efficiency is reduced about six percent.

The system power factor varies from 0.21 at standstill to 0.91 at the upper speed limit of 1500 rpm. The low power factor at standstill is in sharp contrast to the comparatively high power factor measured for transformer-control, as seen from Figure 5. The low system power factor at standstill is a characteristic of thyristor-control and derives from the relatively large reactive impedance presented by the thyristor-control unit.

2.4.2 Input Power Characteristics With Thyristor-Control

Figure 8 presents the measured apparent power S_T, power P_r, displacement power D_p, distortion power Q_d, and the total reactive power, Q_t, plotted as a function of induction motor speed for rated motor current of 44 amperes. Both the thyristor phase delay angle and the dynanometer load were adjusted simultaneously to maintain the stator current constant over the range of motor speeds investigated. Since the true RMS line current was held constant, the input apparent power was approximately constant throughout the test run. The composite set of power characteristics, giving the real and reactive power components for a thyristor-controlled R-L load, provide a comprehensive picture of the distribution of power in this type of power conditioning system. The comparative set of power characteristics for the case of transformer voltage control was given in Figure 6. The thyristor load system, increases with speed over the full range of motor speed examined. Since higher speeds required a reduction in line current and ultimately dynanometer loading, it was not possible to extend the range of motor speeds beyond a higher upper limit. Consequently, the peak in real power which must take place at motor slips smaller than the least value

3. CONCLUSIONS

The output characteristics of a rotary induction motor have been examined in the laboratory using transformer-voltage-control and thyristor-voltage-control. The laboratory study indicates that the mechanical power developed by the motor is approximately equal for the two types of voltage control. Thyristor control does introduce some additional losses due to losses in the silicon rectifiers and losses associated with harmonic currents in the stator and rotor circuits. Since these harmonic currents in a thyristor-controlled induction motor are relatively small at speeds approaching rated slip, the reduction in motor efficiency caused by the distortion of the current waveform is also small in this case. However low motor speeds, and particularly at standstill, thyristor-voltage-control can result in large current waveform distortion and the losses arising from the harmonic currents should be taken into consideration in evaluating the overall system efficiency.

The study of the characteristics of electrical power in transformer-voltage control and thyristor-voltage-control demonstrates several facts concerning these two types of power conditioning systems. In transformer-voltage-control, distortion power is absent and the total input apparent power is distributed between the active power absorbed by the load and reactive displacement powe stored in the circuit. In thyristor-voltage-control, there is additional reactive power by virtue of the distortion power generated by the SCR control unit. In this latter case, the total input apparent power to the system is equal to the 'vector' sum of the real power, reactive displacement power, and the reactive distortion power. If the power factor is computed from the ratio of the real power to apparent power, the result is consistent for both transformer-voltage-control and thyristor-voltage-control. If one determines the system power factor solely from the method requirements the input to the control system the result will be incorrect if distortion power is present in the system. The total reactive power in the electrical system, i.e., the vector sum of displacement power and distortion power, can be found from measurements of

the input apparent power and active power and applying Equation (16). The resulting reactive power plus measured active power comprise the total complex power in the system when distortion power is present. This study also demonstrates the legitimacy of computing distortion power indirectly from measurements of apparent, and reactive displacement powers. This result is important since it means that separate (and somewhat time-consuming) measurements of harmonic current amplitudes are not required to evaluate distortion power.

The report concludes that the effective instrumentation of a thyristor-voltage-control system requires the apparent and the active power to be measured at the input to the control system. The ammeter and voltmeter should be wide-band to measure true RMS line current. At the input terminals to the load, wattmeters may be necessary to measure the real power input to the load if input voltage waveform distortion is present. The information obtained from the above instrumentation will be sufficient to evaluate the complex power quantities at the input to the control system and the real power consumed in the load and the power conditioning system. It should be noted that this study has addressed the case of balanced 3-phase loads. For significant load unbalances, such as encountered in the PTACV, the effects of negative-sequence currents introduces major complexities, not addressed in this study. It is recommended that this effect by part of a future analysis.

REFERENCES

1. Rohr Industries, Report No. 1.6, Power and Propulsion System, Urban Tracked Air Cushion Program, prepared for the Department of Transportation under Contract No. DOT-UT-10031.

2. Derek A. Paice, Induction Motor Speed Control by Stator Voltage Control, IEEE Transactions on Power Apparatus and Systems, Vol. PAS-87, No. 2, February 1968.

3. W. Shepherd, and J. Stamway, The Polyphase Induction Motor Controlled by Firing Angle Adjustment of Silicon Controlled Rectifiers, Paper 147, IEEE International Convention, March 1964.

4. B. Chalmers and B. Sarkar, Induction Motor Losses Due to Nonsinusoidal Supply Waveforms, Proc. IEEE, Vol. pp. 19.

5. E. Klingshirm and H. Jordan, Polyphase Induction Motor Performance and Losses on Nonsinusoidal Voltage Sources, IEEE Transactions on Power Apparatus and System, Vol. PAS-87, No. 3, Marcl 1968.

6. G. Jain, The Effect of Voltage Waveshape on the Performance of a 3-Phase Induction Motor, Proc. IEEE, Vol., pp 561-566, June 1964.

7. T.A. Lipo, The Analysis of Induction Motors with Voltage Control by Symmetrically Triggered Thyristors, IEEE Transactions on Power Apparatus and Systems, Vol. PAS-90 No. 2, March/April 1971.

8. J. Stickler, Effect of Frequency and Spatial-Harmonics on Rotary and Linear Induction Motor Characteristics, Report No. DOT-TSC-UMTA-72-7, prepared for Department of Transportation, Urban Mass Transportation Administration, Washington, D.C. 20590, March 1972.

9. R. Bedford and V. Nene, Voltage Control of the Three-Phase Induction Motor by Thyristor Switching; a Time-Domain Analysis Using the Transformation, IEEE Transactions on Industry and General Applications, Vol, IGA-6, No. 6 Nov/Dec 1970.

10. Donald W. Novotny, A Frederick Fath, The Analysis of Induction Machines Controlled by Series Connected Semi conductor Switches, IEEE Transactions on Power Apparatus and Systems, February 1968.

11. W. Shepherd, On the Analysis of the Three-Phase Induction Motor with Voltage Control by Thyristor Switching, IEEE Transactions on Industry and General Applications, Vol. IGA-4, No. 3, May/June 1968.

12. A. Schmidt, Jr., Power Factor of Rectifiers, AIEE Winter General Meeting, New York, N.Y., February 1958.

13. Michael S. Erlicki, David Schrieber, Joseph Ben Uri, Power Measurement Errors in Controlled Rectifier Circuits, IEEE Transactions on Industry and General Applications, July/August 1966.

14. K. Neil Stanton, Instrumentation for Thyristor Control, IEEE Transactions on Industry and General Applications, Vol. IGA-4, No. 6, November/December 1968.

15. Schaeffer, "Rectifier Circuits; Theory and Design", John Wiley & Sons, New York, 1965.

16. W. Shepherd and P. Zakikhani, Suggested Definition of Reactive Power for Nonsinusoidal Systems, Proc. IEEE, Vol 119, No. 9, September 1972.

17. Frank L. Raposa, Power Conditioning for High Speed Ground Transportation Vehicles, presented at the joint IEEE Power Processing and Electronics Specialist Conference/25th Power Sources Symposium, Atlantic City, N.J. May 23, 1972.

18. R.A. Cacossa, A Survey of Variable Voltage Power Conditioners for Application to the Tracked Air Cushion Vehicle, Report No. DOT-TSC-UMTA-71-4, prepared for Department of Transportation, Urban Mass Transportation Administration, Washington, D.C. 29590, March 1971.

19. IEEE Subcommittee on Thyristor AC Power Control, Proposed IEEE Standard for Thyristor AC Power Controllers, Seventh Annual Meeting of IEEE Industry Applications Society, Philadelphia, Pennsylvania, Oct. 9-12, 1972.

APPENDIX

THYRISTOR VARIABLE VOLTAGE POWER CONDITIONER TEST SETUPS AND APPARATUS

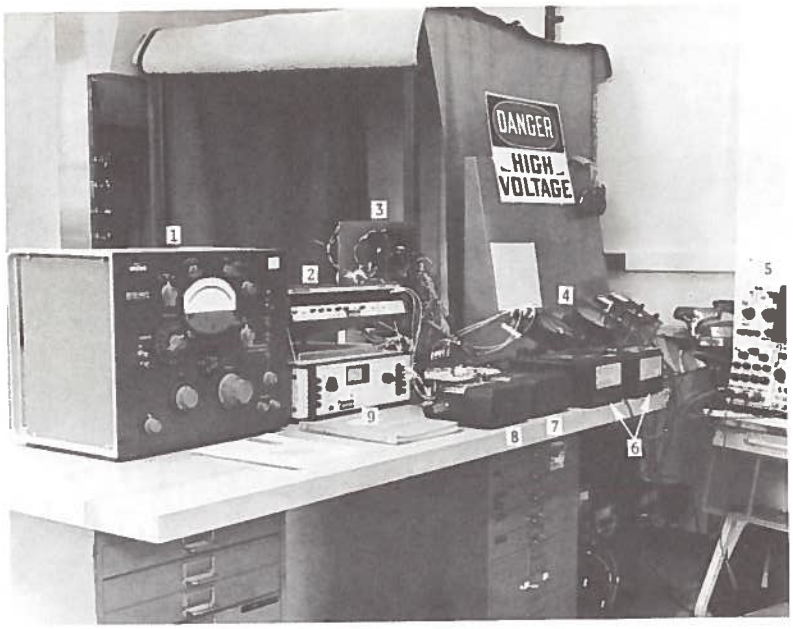

LEGEND

1. Wave Analyzer General Radio Model 1900
2. Digital Voltmeter Hewlett Packard Model 3430A
3. TSC Thyristor Controlled Variable Voltage Power Conditioning Unit
4. 90HP Absorption Brake Dynamometer Stuska Model 90413
5. Dual Beam Oscilloscope Tektronix Type 556
6. Wattmeters Hallmark Standards Model HWP-2
7. D.C. Voltmeter Weston Model 901
8. A.C. Voltmeter Weston Model 904
9. RMS Digital Converter Weston Rotek Model PR840
0. TSC Hall Effect Device True RMS Current Transduces (Not Shown)
1. Variac General Radio Type W50 (Not Shown)
2. Howell High Slip 15HP 208-Volt 3Ø Induction Motor (Not Shown)

Figure 9 Laboratory Arrangement

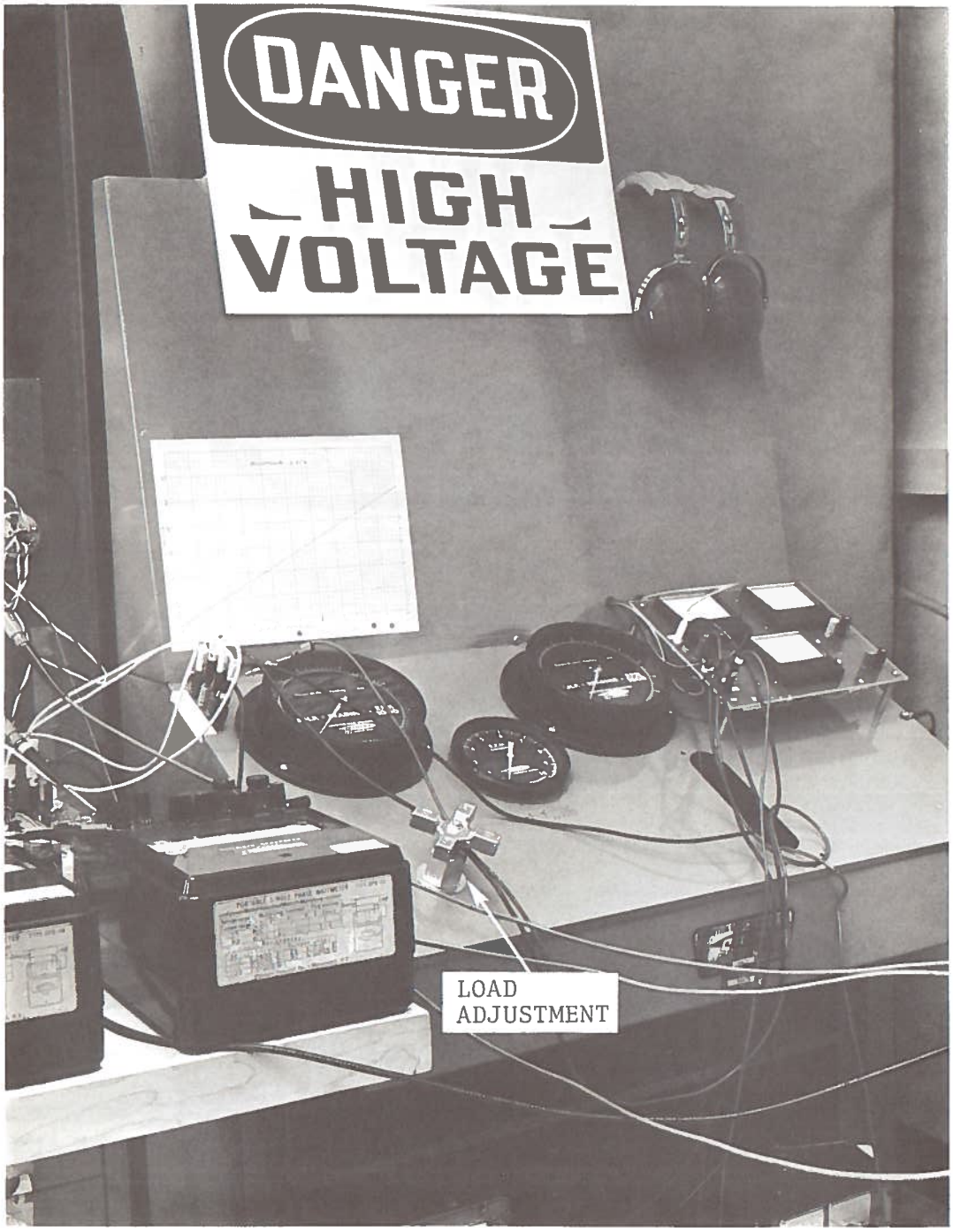

Figure 10 Absorption Brake Dynamometer Control Panel

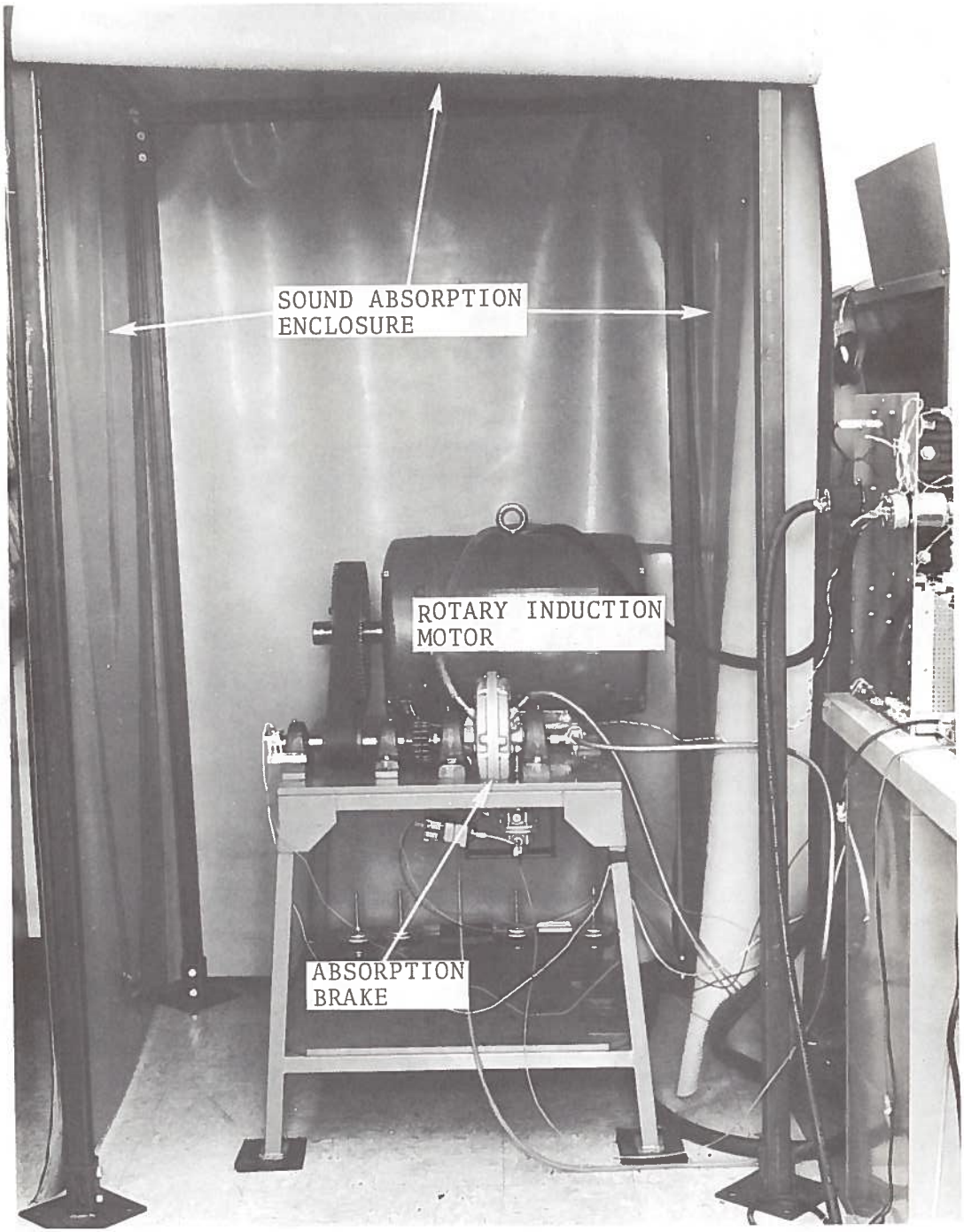

Figure 11 Load Test Apparatus

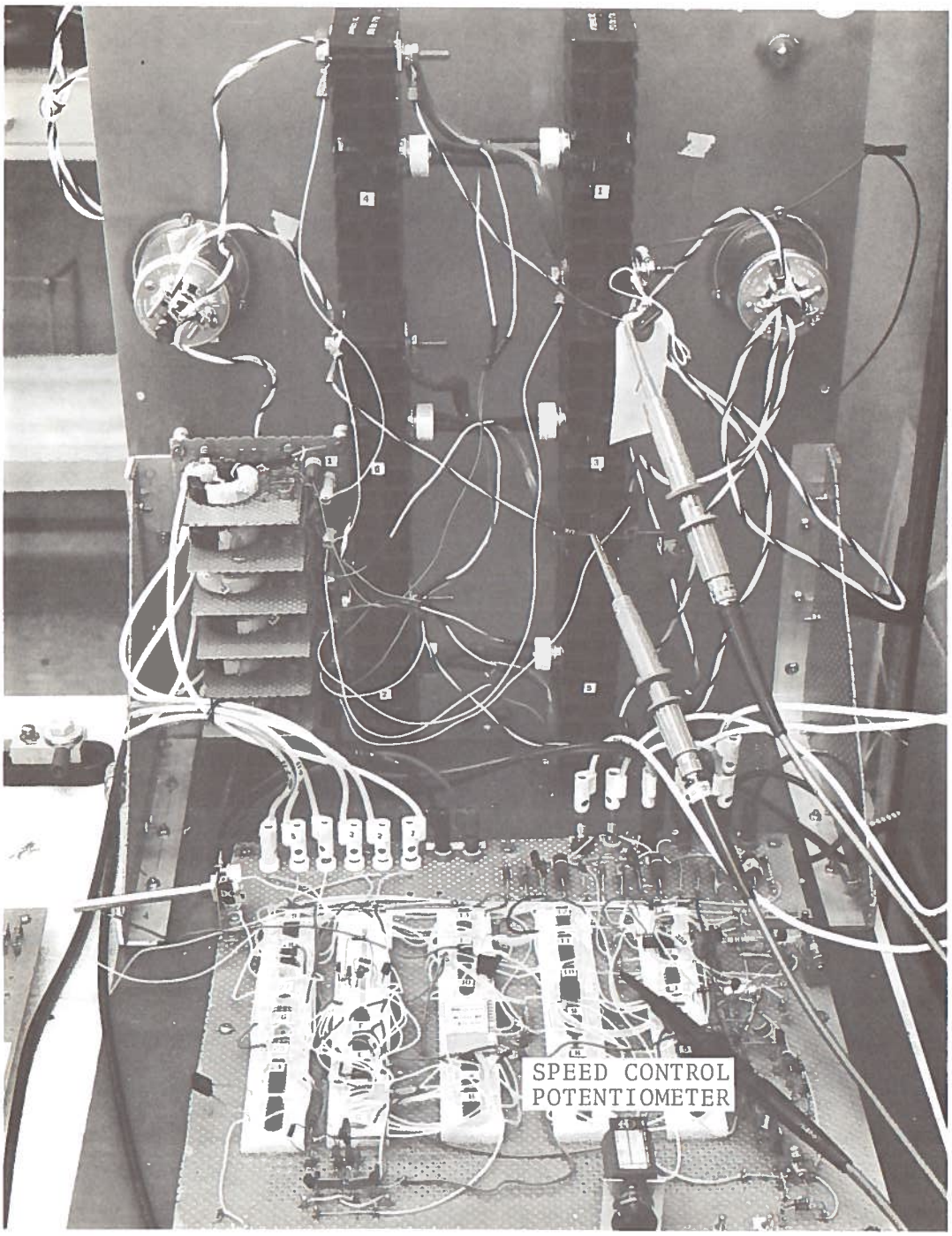

Figure 12 TSC Variable Voltage Power Conditioning Unit (VVPCU)

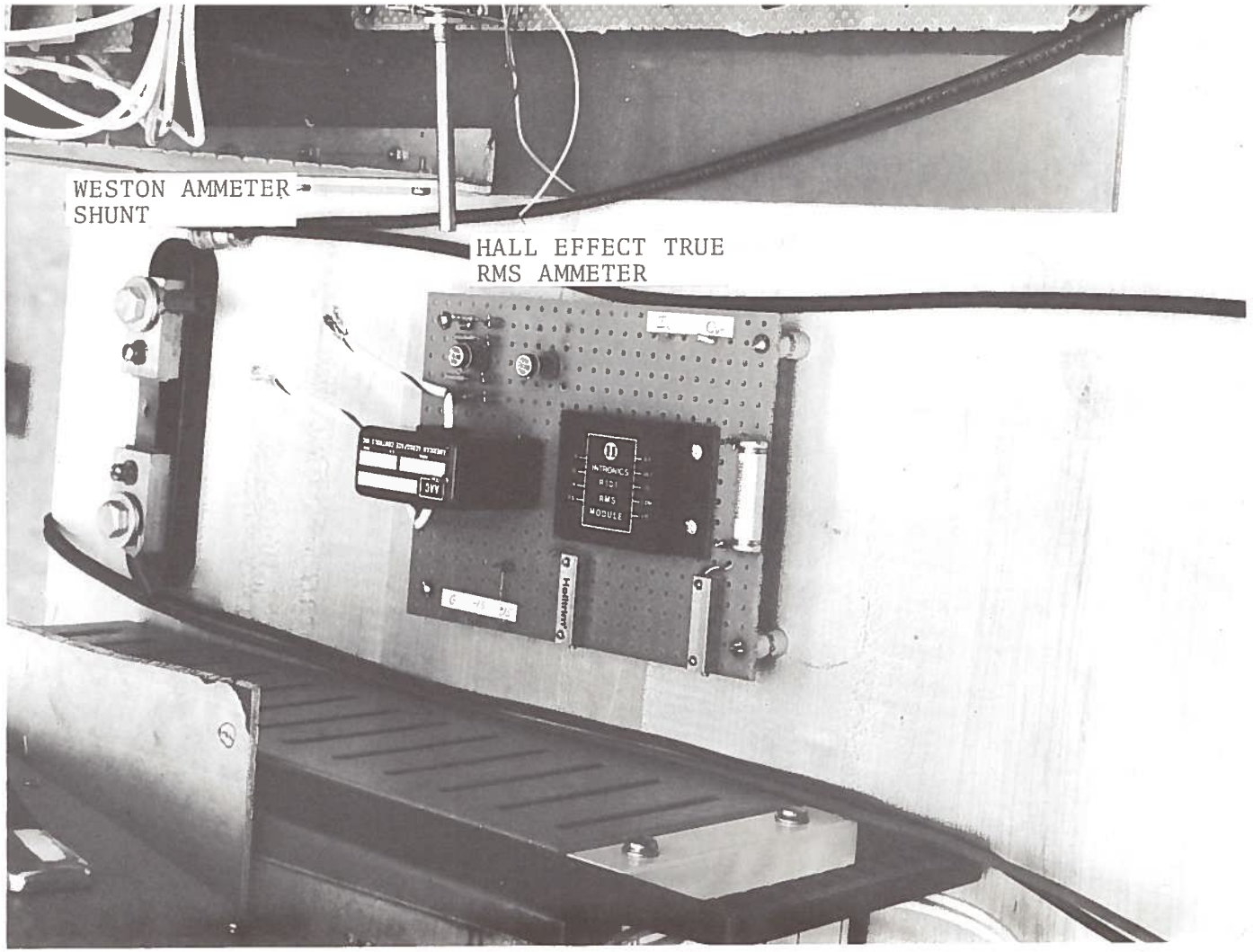

Figure 13 Current Meter Test Apparatus